Available online at www.sciencedirect.com
SCIENCE DIRECT
Journal of Catalysis 227 (2004) 470–478
JOURNAL OF CATALYSIS
www.elsevier.com/locate/jcat

Liquid-phase catalytic activity of sulfated zirconia from sol–gel precursors: the role of the surface features

S. Ardizzone [a,*], C.L. Bianchi [a], G. Cappelletti [a], F. Porta [b]

[a] *Department of Physical Chemistry and Electrochemistry, University of Milan, Via Golgi 19, I-20133 Milan, Italy*
[b] *Department of Inorganic, Metallorganic and Analytical Chemistry, University of Milan, Via Venezian 21, 20133 Milan, Italy*

Received 16 June 2004; revised 26 July 2004; accepted 27 July 2004

Available online 17 September 2004

Abstract

ZrO_2–SO_4 powders were prepared through a single step sol–gel reaction by modulating the conditions of the alkoxide hydrolysis and polycondensation steps. Sulfuric acid or $(NH_4)_2SO_4$ was employed as the sulfating agent. The samples were calcined at 890 K and characterized as to phase composition crystallinity (XRD) and surface area porosity (BET method). Surface functionalities were investigated by TGA/FTIR, FTIR, DRIFTS, and XPS analyses. The liquid-medium catalytic activity was tested in the esterification of benzoic acid to methylbenzoate. The role played by the conditions of the sol–gel reaction, in affecting the surface state and the catalytic properties of the powders, is discussed.

Keywords: Sulfated zirconia; Liquid media catalyst; Surface functionalities; XPS; Sol–gel

1. Introduction

In recent years sulfate-doped zirconia (SZ) powders have been the object of great interest as solid catalysts for several reactions and, mainly, for low-temperature *n*-alkane isomerization [1–17]. The treatment of the oxide hydrous precursor with sulfates results, in fact, in a very strong increase in the acidity of the powders and, consequently, in a very promising activity toward a large number of acid-catalyzed reactions. Besides affecting the acid character of the samples, sulfates produce several modifications in the features of the oxide concerning: (i) phase composition, (ii) degree of crystallinity, (iii) extent of surface area, (iv) degree of porosity, (v) surface state, etc. [2,3,8,9]. Much work has been done, in the literature, regarding these latter topics and some controversial results have been reported particularly concerning the stoichiometry of the sulfur-containing surface species and the Lewis or Brønsted nature of the acidic active sites [18–20]. The presence in the literature of divergent results concerning various aspects of SZ systems is, at least in part, due to the manifold features of these materials, and to the close interplay between different parameters introduced by the preparative steps.

Sulfated zirconia is classically synthesized by precipitation of zirconium hydroxide from salt solutions, subsequent impregnation with a sulfating agent, and final calcination at temperatures in the range 720 and 970 K, in order to obtain a catalytically active crystalline compound [2,5,6].

In recent years a new synthetic approach, the sol–gel route, has been proposed for the synthesis of SZ catalysts [3,15,21,22]. The sol–gel preparation of an oxide implies the hydrolysis of a metal alkoxide to form the hydroxide and the subsequent polycondensation to give the gel. Both reactions can be catalyzed either by strong acids or by bases. In the specific case of the sol–gel synthesis of sulfated zirconia, a sulfating agent can be introduced during the gel formation allowing the impregnation step to be avoided and the overall procedure to be greatly simplified.

* Corresponding author. Fax: +390250314300.
E-mail address: silvia.ardizzone@unimi.it (S. Ardizzone).

0021-9517/$ – see front matter
doi:10.1016/j.jcat.2004.07.030

In the case of sol–gel reactions several parameters intervene in imposing the features of the product, both concerning the "chemical" composition of the reacting mixture and also the physical conditions adopted for the reaction (temperature and time length of the hydrolysis–condensation steps, gel drying conditions, etc.). Consistently with this latter considerations we have observed, in the case of SZ catalysts prepared by the sol–gel route, definite effects on the features of SZ catalysts and their activity toward *n*-butane isomerization provoked by the conditions adopted for the solvent removal at the end of the gelling reaction [3]. Further, more recently, we have evidenced the role played by the variation of the water/alkoxide ratio, in the starting preparative mixture, on the catalytic activity of SZ catalysts in liquid media [22].

The major part of the reported sol–gel syntheses of SZ catalysts is performed by adopting an acid catalyst for the polycondensation reaction, mainly sulfuric acid which can act, at the same time, as the source of sulfates [23,24]. The present work is devoted to the investigation of the role played under the conditions adopted for the hydrolysis and condensation reactions leading to the gel formation (either acid or basic catalysis) and by the nature of sulfating agent (H_2SO_4 or $(NH_4)_2SO_4$) on the physicochemical features of the SZ powders. The samples, submitted to a thermal treatment, are characterized with respect to the structural and morphological features. Different surface analyses (XPS, FTIR, DRIFTS) are employed to estimate the possible effects provoked by the variation of the preparative conditions on the surface state of the oxide. The role played by the surface conditions on the catalytic activity of the powders is tested with respect to the esterification of benzoic acid with methanol.

2. Experimental

All the chemicals were of reagent grade purity and were used without further purification; distilled water passed through a Milli-Q apparatus was used to prepare solutions and suspensions.

2.1. Sample preparation

SZ powders were prepared by the sol–gel technique using zirconium *n*-propoxide, $Zr(OPr)_4$ as a precursor. To a starting solution prepared by mixing $Zr(OPr)_4$, the sulfating agent (either sulfuric acid or $(NH_4)_2SO_4$), and i-PrOH, water was added dropwise under vigorous stirring at 298 K. The molar ratio between the sol–gel reaction catalyst ($C_{sol-gel}$) and the alkoxide was varied from the maximum value of 0.21 to 0, either in the acid or in the alkaline direction. Acid-promoted precursors were prepared by using nitric acid; for the sake of comparison samples, at the 0.21 $C_{sol-gel}$/alkoxide ratio, were obtained also by using as the promoting acid H_2SO_4. When comparing nitric and sulfuric acid the proton concentration was kept constant; also the amount of sulfates, either from sulfuric acid or from $(NH_4)_2SO_4$, was the same for all preparations (molar ratio $SO_4/Zr = 0.21$). The base-promoted precursors were obtained by adding to the reacting mixture NaOH. The water/alkoxide molar ratio was kept constant at 30. The gels were dried as xerogels at 353 K at atmospheric pressure for 15 h. The xerogels were calcined at 890 K for 5 h in an oven under an oxygen flux.

SZ samples are labeled as SZa for acid catalysis of the sol–gel reaction, SZ for spontaneous pH, i.e., no acid or base added, and SZb for alkaline catalysis. In the case of the acid-catalyzed samples N stands for nitric acid and S stands for sulfuric acid. When not indicated the $C_{sol-gel}$/alkoxide ratio is 0.21. For example SZaN represents a sample prepared by an acid reaction with nitric acid, with a $C_{sol-gel}$/alkoxide ratio of 0.21; SZaN0.5 represents a sample prepared by an acid reaction with nitric acid, with a $C_{sol-gel}$/alkoxide ratio of 0.105; SZb represents a sample prepared by an alkaline reaction with sodium hydroxide, with a $C_{sol-gel}$/alkoxide ratio of 0.21.

2.2. Sample characterization

Structural characterization of the powders was performed by X-ray diffraction, using a Siemens D500 diffractometer, using Cu-K_α radiation in the 10–80° 2θ angle range. The fitting program of the diffraction lines was a particular Rietveld program [25,26], named QUANTO [27], devoted to the automatic estimation of the weight fraction of each crystalline phase in a mixture. The mean dimension, d, of crystallites was obtained by elaborating the most intense X-ray diffraction line of each phase by the Scherrer equation.

Specific surface areas were determined by the classical BET procedure using a Coulter SA 3100 apparatus.

XPS analyses were obtained using an M-probe apparatus (Surface Science Instruments). The source was monochromatic Al-K_α radiation (1486.6 eV). A spot size of 200 × 750 μm and a pass energy of 25 eV were used. 1s level hydrocarbon–contaminant carbon was taken as the internal reference at 284.6 eV. The fitting procedure of the O 1s spectral components was performed, as reported previously [2,3,6,8,9,14], on the grounds of tabulated and experimental BE and of FWHM values obtained from a standardization method on pure ZrO_2 and $Zr(SO_4)_2$. The accuracy of the reported binding energies (BE) can be estimated to be ±0.2 eV.

2.3. Spectroscopic characterization

TGA/FTIR measurements have been performed by monitoring gas evolution using a JASCO-FTIR spectrophotometer Model 360 coupled with a Dupont Model 951 thermogravimetric analyzer. During the sample reaction, the evolved gases were transferred through a stainless-steel

tube heated at 383 K to a 15-cm-long multipass White cell equipped with KBr windows reaching an optical path of 120 cm. An infrared spectrum was collected automatically, simultaneously with the thermogravimetric analysis, every 60 s. The experimental conditions used for the analyses were: N_2 atmosphere, gas flow rate, 60 ml min^{-1}; temperature scanning, 10 K min^{-1} in the range ambient temperature—923 K. The continuous monitoring at 1622 cm^{-1} (to which corresponds the IR absorption due to water) and at 1359.1 cm^{-1} (to which corresponds the IR absorption due to sulfur trioxide) has produced evolution curves as a function of the temperature.

FTIR spectra of solid samples were recorded on Avatar 360 FTIR spectrophotometer at room temperature in the air. DRIFTS (diffuse reflectance infrared Fourier transform spectroscopy) of finely ground samples, loaded in a homemade DRIFTS reaction chamber, were recorded at 4 cm^{-1} resolution on a Digilab FTS-60 spectrometer equipped with a KBr beam splitter and a N_2 cooled linearized broadband MCT detector operating between 400 and 4000 cm^{-1}. The treatment at 723 K was carried out under He flow (50 ml min^{-1}) for 0.5 h.

2.4. Catalytic tests

The esterification reaction of benzoic acid to methylbenzoate was chosen to test the catalytic efficiency of the SZ samples in liquid media. Details of the experimental procedure have been reported previously [28]. Briefly, it can be recalled that, as the esterification reaction is an equilibrium one, the temperature of the process was fixed at 433 ± 1 K in order to shift the equilibrium to the products, by the continuous distillation of the water produced during the reaction. As the boiling point of methanol is 340 K, the operative way may be described as a modified "batch process", where the reagents are put altogether in the reactor and methanol is continuously added and taken off together with water. The amount of 2.5 g of catalyst was added into the reactor, and samples of 5 ml of the reaction mixture were picked up to test the catalytic performance as a function of the reaction time.

3. Results and discussion

3.1. Structural and morphological features

The phase composition and crystallite sizes were determined for all the calcined samples by XRD measurements. The relative enrichment in the different zirconia polymorphs was determined by the Rietveld method, estimating the crystallite sizes by the Scherrer equation. Fig. 1 shows the X-ray diffractograms of three representative samples. In the figure only the 100% intensity lines of tetragonal and monoclinic zirconia, respectively, are labeled. The other unlabelled lines represent the less intense signals pertaining to

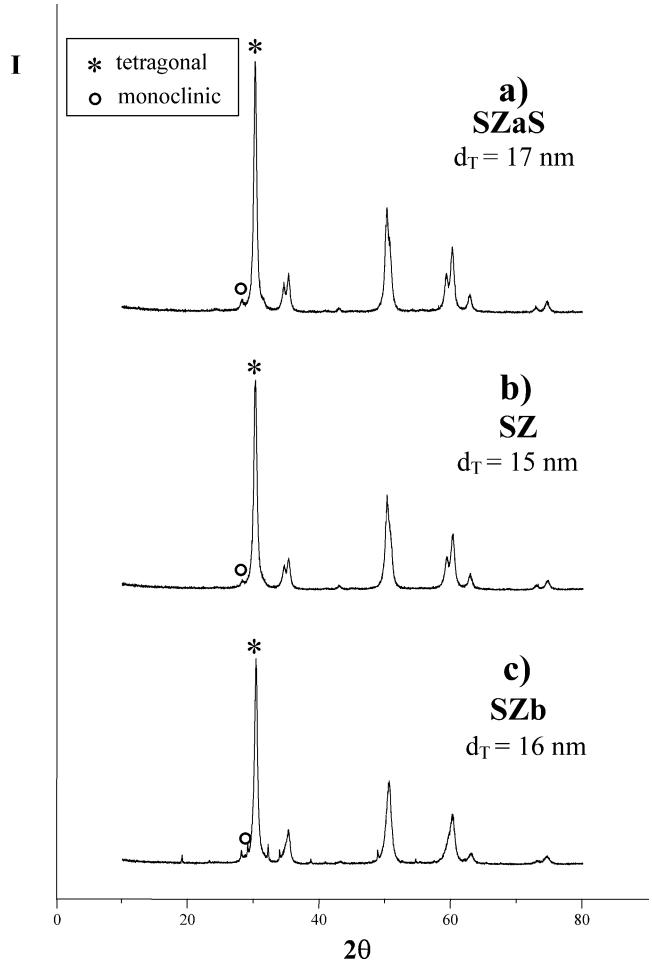

Fig. 1. Powder X-ray diffraction lines of different samples calcined at 890 K. The size of the tetragonal zirconia crystallites (d_T) was estimated by the Scherrer equation.

the same structures. In the three cases, the tetragonal zirconia polymorph is the main component in the presence of minor monoclinic amounts. No significant lines of either Na_2SO_4 or Na_2O can be appreciated. The observed structural features are in agreement with the major part of literature results. In fact the "doping" of zirconia with sulfates is generally reported to reduce the crystallite sizes and to stabilize the tetragonal polymorph [2,5,18]. The variation of either the reaction catalyst or the nature of the sulfating agent do not seem to provoke any definite trend with respect to the phase composition of the calcined samples.

Table 1 reports the surface area (S) values of the samples together with the total pore volume and the micropore volume (when present). All the S values range around 80 $m^2\,g^{-1}$ with the sole exception of SZaN which presents a slightly lower area. While the surface areas do not seem to be appreciably affected by the preparation route, the porosity features show some trend on the adopted pH conditions. Fig. 2 shows that the total pore volume increases for the neutral-basic samples and is accompanied by a shift of the pore-size distribution to larger values. A similar effect of increase in the pore size distribution due to the pH conditions

Table 1
Sample surface area and total pore volumes

Sample	S_{BET} ($m^2\,g^{-1}$)	Pore volume ($ml\,g^{-1}$)	Micropore volume ($ml\,g^{-1}$)
SZaS	84.5	0.056	0.0012
SZaN	71.1	0.066	0.0000
SZaN0.5	85.8	0.058	0.0000
SZ	79.0	0.108	0.0000
SZb0.5	83.7	0.167	0.0152
SZb	79.1	0.107	0.0118

The micropore volume was estimated by the *t* plot.

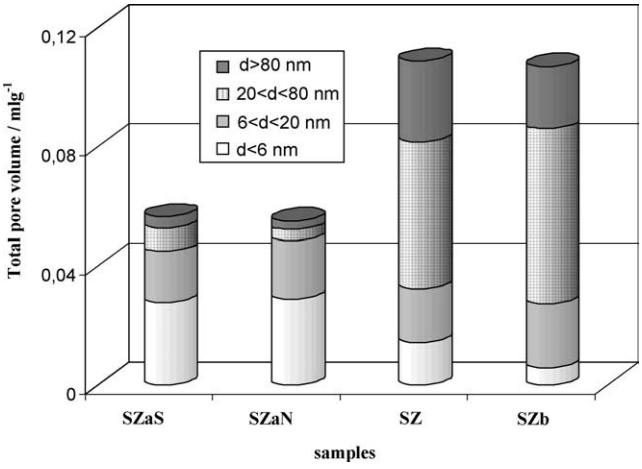

Fig. 2. Total pore volume and relative volume distribution.

of the catalysis is reported in the case of silica aerogels [29] and of silica–zirconia mixed oxides [30]. Moreover, the two alkaline samples show the occurrence of an appreciable extent of microporosity (Table 1, third column). The variation of the conditions adopted for the sol–gel reaction does not affect the phase composition of the samples or the surface area but the adoption of alkaline conditions provokes significantly different textural properties. The alkaline hydrolysis in the sol–gel preparation of an oxide is, in fact, reported to be much slower than the corresponding one performed under acid conditions and this could have given rise to a more porous network and to a significant extent of micropores. Further it is possible that, in the present case, the effects of the conditions of preparation on the pore structure and surface area are compressed by the drying of the precursors as xerogels.

3.2. XPS determinations

Survey XPS spectra were recorded for all samples. No significant presence of impurities was observed, except for the ubiquitous carbon contaminant. In the case of the latter element, only the C 1s peak at 284.6 eV (due to –CH– species) was present.

The peak of the Zr 3d doublet was found to be in any case regular with BE values (182.2–184.6 eV) consistent with literature data relative to Zr(IV) species in the oxide phase. The distortion of the Zr 3d peak of ZrO_2 samples upon sulfation has been reported in the literature for samples calcined at temperatures lower than the present ones and to be restored to that of a regular doublet for temperatures around 900 K [2,6,8,9].

The spectrum of S 2p was never intense, due to the low intrinsic sensitivity factor of this element. Except for the SZb sample, the *S* peak could be fitted by a single component at BE = 169.3 eV, (Fig. 3a) in agreement with that

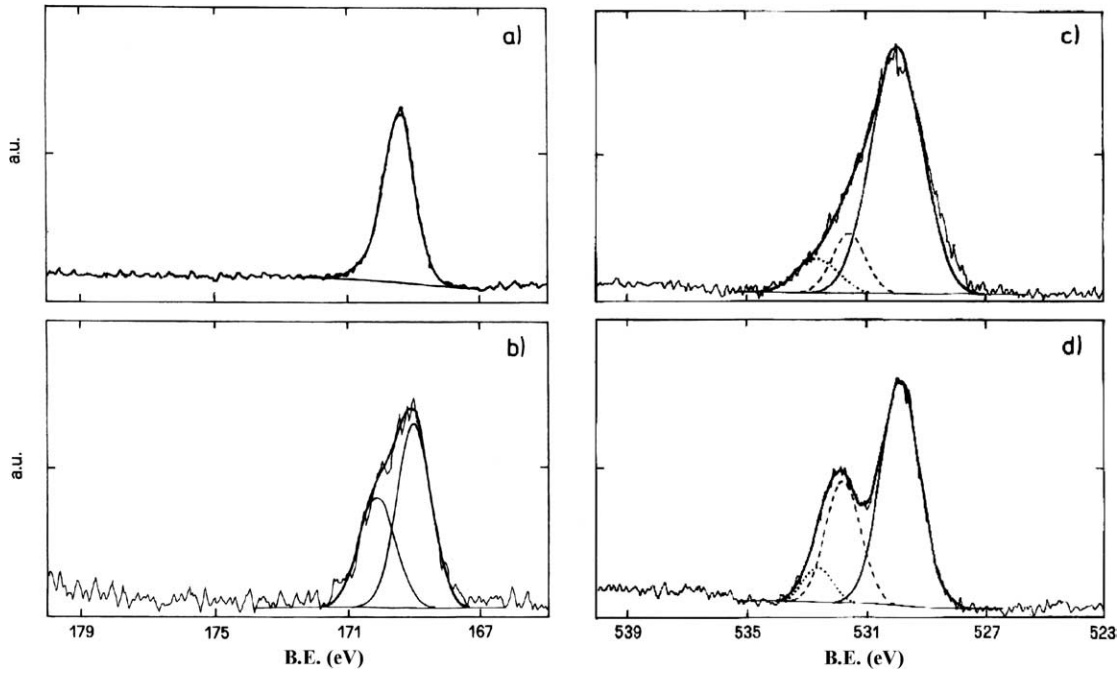

Fig. 3. XPS region of S 2p: (a) SZb0.5 and (b) SZb; XPS O 1s region; (c) SZaN and (d) SZb.

Table 2
XPS atomic ratios of the surface species of the 890 K calcined samples obtained under the different conditions of the sol–gel reaction

Sample	O/Zr	OH/Zr	O/S	S/Zr	Na/Zr	Na/S
SZaS	2.3	0.40	17.2	0.13	–	–
SZaN	2.2	0.40	15.6	0.15	–	–
SZ	2.1	0.35	15.8	0.14	–	–
SZb0.5	2.2	0.25	16.6	0.14	0.12	0.57
SZb	2.7	0.18	10.4	0.26	0.20	2.10

expected for sulfur in sulfates and consistent with previous results relative to other SZ samples [2,6,8,22]. The shape of the sulfur peak of the most alkaline sample (SZb, Fig. 3b) is definitely unusual. The presence of two different components is clearly distinguishable, the first at binding energies comparable to those of the other samples and the second at higher BE. This second component shows the formation, to relevant amounts, of a different sulfur-containing species. It is interesting to observe (Table 2) that SZb shows also the larger sulfur amount, almost twice that of the other samples. Table 2 further shows that in the case of the two alkaline samples Na species are present at the surface and that this occurs to a much larger extent in the case of SZb. The presence of Na and the value of the BE suggests that the second component of the sulfur peak, in the case of SZb, could be the result of the enrichment-segregation at the surface of Na_2SO_4. It is relevant to mention that bulk Na_2SO_4 is not appreciable in X-ray diffractograms and that no soluble product is released from the suspension in water of the present catalysts. The less alkaline sample, SZb0.5, shows a regular sulfur peak and a much lower Na amount at the surface.

The oxygen 1s peak, in the case of SZ catalysts, shows in any case the presence of more than one species. The fitting procedure of O 1s spectral components (Fig. 3c) was adopted previously [2,3,6,8,9,14] and is based on BE values present in the literature and verified by us on reference materials (ZrO_2, $Zr(SO_4)_2$); the main component, at lower binding energies, is assigned to reticular O^{2-} in the oxide (530.0 eV), the second component is attributed to oxygen in sulfates (531.6 ± 0.5 eV), and the third component at higher BE is due to surface OH groups (532.6 ± 0.4 eV). The shape of the peak is generally broad (Fig. 3c); Table 2 shows that, in passing from the acid to the base-promoted samples, the OH/Zr atomic ratios decrease. In the case of SZb the O 1s peak presents a different shape possibly due to a much larger component attributable to oxygen bound to sulfur. Also the O/Zr atomic ratio of SZb is larger than for the other samples (Table 2).

The amount of Na species localized at the surface in the case of SZb is large and larger than the total amount of sulfur. Apparently Na species, added to the sol–gel reacting mixture as NaOH, have undergone surface segregation during calcination in a manner similar to what occurs for sulfates [2,22]. It is important to note that the calcined sample are totally insoluble and that no release of sodium compounds or of other species occurs. The speciation of Na at the surface can be manifold. The presence as Na_2SO_4 is supported by the BE of the second component of the sulfur peak of SZb. The further presence of Na_2O cannot be excluded. The BE of the oxygen peak in Na_2O (529.7 eV) [31] falls in the same region of the ZrO_2 reticular oxygen component and would therefore not be appreciable singularly.

3.3. Spectroscopic measurements

TGA-FTIR experiments, on the sample precursors, were performed under N_2 as described in the experimental section. The presence of SO_3 and water was detected in all samples, by monitoring the absorbance at 1359.1 and 1622 cm^{-1}, respectively; these results are in agreement with literature data [10] obtained on SZ catalysts, prepared by different procedures, by mass spectroscopy of the gases evolved during the thermal treatment.

FTIR spectra of the present SZ catalysts (not reported for reasons of space) showed the hydration of all the samples giving rise to a strong, broad, and unresolved band in the 3600–3000 cm^{-1} region, assigned to physisorbed and possibly coordinated water, accompanied by a broad band close to 1630 cm^{-1} that can be ascribed to the bending mode (δ_{HOH}) of coordinated molecular water. The occurrence of strong interactions between SZ catalysts and water is well known and amply documented in the literature [2,19,20]. Fig. 4 reports the comparison between the DRIFT spectra of SZaN sample, under the as-prepared conditions, and of the same sample after submitting it to a pretreatment at 723 K. In the case of the sample under the as-prepared conditions (curve a), the bands assignable to the S=O double bonds are not evident as awaited in the excess of water while in the case of the sample submitted to the thermal pretreatment (curve b), two sharp bands in the 2000–900 cm^{-1} region, located respectively at 1392 and 1375 cm^{-1} become apparent. The position

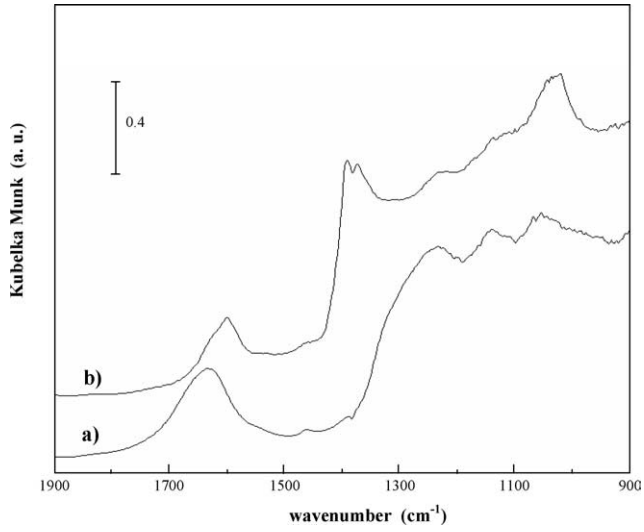

Fig. 4. DRIFT spectra of SZaN sample. (a) Sample as prepared, and (b) sample after treatment at 723 K for 30 min in a He stream.

of the bands, which are attributed to the stretching modes of S=O groups, are in full agreement with literature data of SZ samples, prepared by variable procedures, and submitted to thermal activation treatments [32–35].

In gas-phase catalytic experiments, SZ catalysts are generally submitted to thermal activating pretreatment, mainly aimed at removing physi- and chemisorbed water [2,3]. In the case of liquid-phase catalysis the catalysts are generally added to the reaction mixture under the as-prepared conditions [2,30]. No thermal pretreatment of the SZ powders, to be used as catalysts for the liquid phase reaction, is therefore performed in the present case. Analogously also the DRIFTS is performed for the samples under the as-prepared conditions, in order to produce a direct comparison between surface state of the samples, prepared under the different conditions, under the actual catalytic reaction conditions. Although the bands assignable to S=O bonds are not appreciable, the spectra (Fig. 5) show distinctive features: the spectra of SZaN and SZ (curves b and c, acidic and neutral-synthesized samples) show a fully comparable trend and their difference from SZb (alkaline-catalyzed sample, a) is apparent. The spectra of SZaS and of SZb0.5 (not reported for the sake of clarity) are totally comparable with SZaN and SZb, respectively. In the low frequency portion of the spectrum, the major peaks appear in the 1250–850 cm^{-1} region; in c, the bands are detected at 1252, 1139, 1052, and 995 cm^{-1}, in b at 1259, 1139, 1052, 1031, and 990 cm^{-1}, while a broad band at 1187 cm^{-1} (1118 cm^{-1} shoulder) with a small peak at 996 cm^{-1} is appreciable in a. In agreement with Ref. [2] the stretching modes of sulfate group ($\nu_{S=O}$ and ν_{S-O}) can be expected to display a small separation when the surface is highly hydrated; i.e. the sulfate spectral pattern could change from the typical 1400–850 to the 1250–850 cm^{-1} region. This separation depends on the ionic/covalent characters of sulfates [2,33]. The covalent character depends on the surface dehydration degree [36] but also on the feasible coordination of oxygen atom(s) to the Zr centres (that reduces the S=O bond order). Several binding modes are proposed in the literature for sulfate in SZ catalysts. Yamaguchi [11] proposed that the sulfate chelates one Zr by a double oxygen bond attracting electrons away and making it a strong Lewis acid. Clearfield et al. [5], instead, suggested that sulfur bridges across two zirconium atoms and that by water sorption Lewis acid sites are converted to Brønsted acid sites. Benaissa et al. [37], by HRTEM characterizations, observed two- or threefold coordinations for the sulfate groups bound to zirconia crystallites. In the present case a detailed analysis of the surface-binding modes is thwarted by the excess water and is out of the scope of the paper. However the shape of spectrum a suggests the presence of coordinated sulfate with a higher symmetry with respect to those in c and b. Further the shape of the peak suggests a strong similarity between the Zr centers, coordinated to sulfate, and their proximal neighbors on the surface. In the case of the alkaline samples, therefore, the capability of sulfates to attract electrons away from zirco-

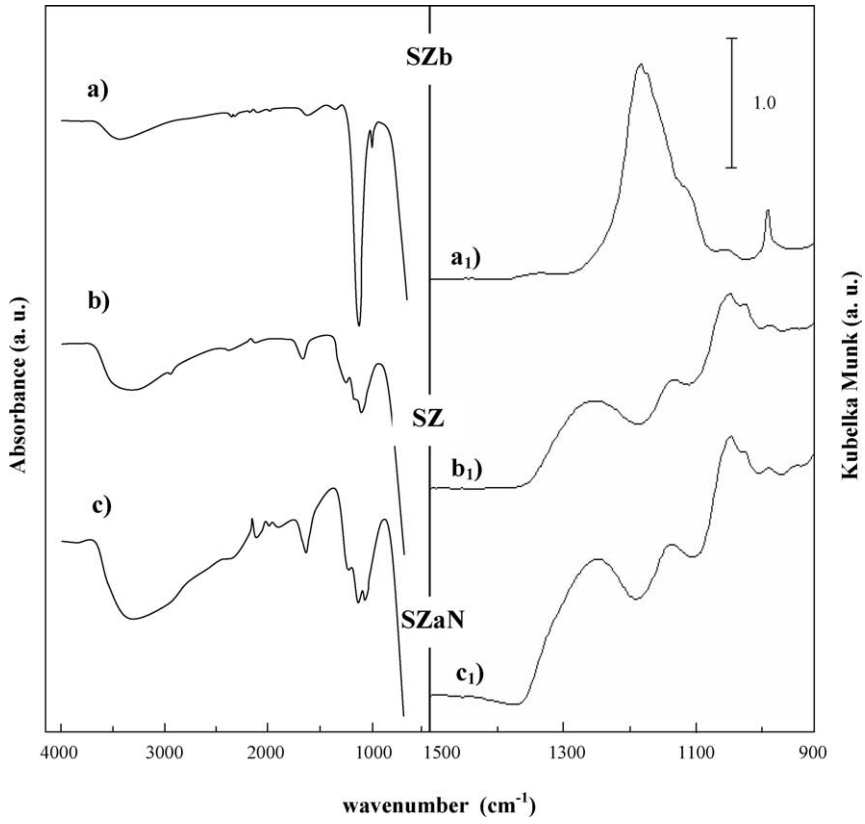

Fig. 5. FTIR and DRIFT spectra of SZb (a and a_1, respectively), SZ (b and b_1, respectively), and SZaN (c and c_1, respectively) samples.

nium would be reduced leaving Zr surface sites less active. The spectrum of SZaN confirms the presence of uncoordinated Na_2SO_4 (shoulder at 1118 cm^{-1}, a) as observed by XPS spectroscopy.

3.4. Catalytic tests

The activity of SZ systems as heterogeneous catalysts in liquid media has been less investigated with respect to gas-phase reactions. The successful SZ-catalyzed acylations of aromatic ketones [38] and the appreciable activity of SZ systems for esters hydrolysis were reported [39,40].

In the present tests, the powders have been used as heterogeneous catalysts for the esterification of benzoic acid with methanol [2]. Leaching tests, aimed at verifying the possible release of sulfates from the catalysts during the course of the reaction, were in any case negative, allowing the catalysis to be considered as heterogeneous [28].

Fig. 6 reports the conversion to methyl benzoate obtained after 8-h reaction time as a function of the conditions adopted in the sol–gel preparation of the oxide precursor. All the xerogel precursors were fired at 890 K. The reaction profile (conversion vs time) is reported as an inset to Fig. 6. The selectivity is 100%. The catalysts, withdrawn from the reacting mixture, at the end of the reaction test, and submitted to "washing" cycles show a much larger C/Zr ratio than fresh samples [2].

The absolute conversion (Fig. 6) shows an S-shaped trend, with maxima values for the two samples obtained with the highest acid/alkoxide ratio. These two samples, prepared respectively from sulfuric acid and nitric acid (plus ammonium sulfate), do not show appreciable differences in their catalytic behavior. The activity of the catalysts decreases with lowering the acid amount in the reaction and the samples obtained by alkaline promotion of the sol–gel reaction show the lowest conversion.

The trend apparent in Fig. 6 can be, hardly, attributed to a variation in the active surface area of the catalysts in the reaction medium. The surface area of the catalysts (Table 1) in fact is not affected by the conditions adopted for the catalyst precursor preparation. In the case of the "alkaline" samples, however, a role played by the morphology of the catalysts on the decrease of the catalytic conversion cannot be excluded. Samples SZb and SZb0.5, in fact, show the presence of an appreciable amount of micropores. The sizes of both benzoic acid (d, 0.4 nm) and the benzoate (d, 0.7 nm) [41] are very small and the diameter of the pores is larger than three times the molecule diameter; however, it cannot be totally excluded that the fraction of surface area relative to micropores represents a less accessible region for the reacting species.

However, the reduction of accessible surface area cannot be considered the sole origin of the trend reported in Fig. 6. The decrease in activity is, in fact, large and the absolute value of the conversion is comparable to the one obtained for the reaction in the absence of a catalyst [28].

The "blocking" of the surface sites due to the presence of Na_2SO_4 cannot be considered as the origin of the trend in Fig. 6. The salt in fact is uncoordinated and its amount varies largely from sample SZb0.5 to SZb while the catalytic conversion is hardly different between the two samples.

It is the opinion of the authors that the major component affecting the catalytic activity of the present SZ catalysts is the actual surface state as apparent in the DRIFTS characterization. The higher symmetry of coordinated sulfates, apparent for the alkaline samples, implies a lower electron

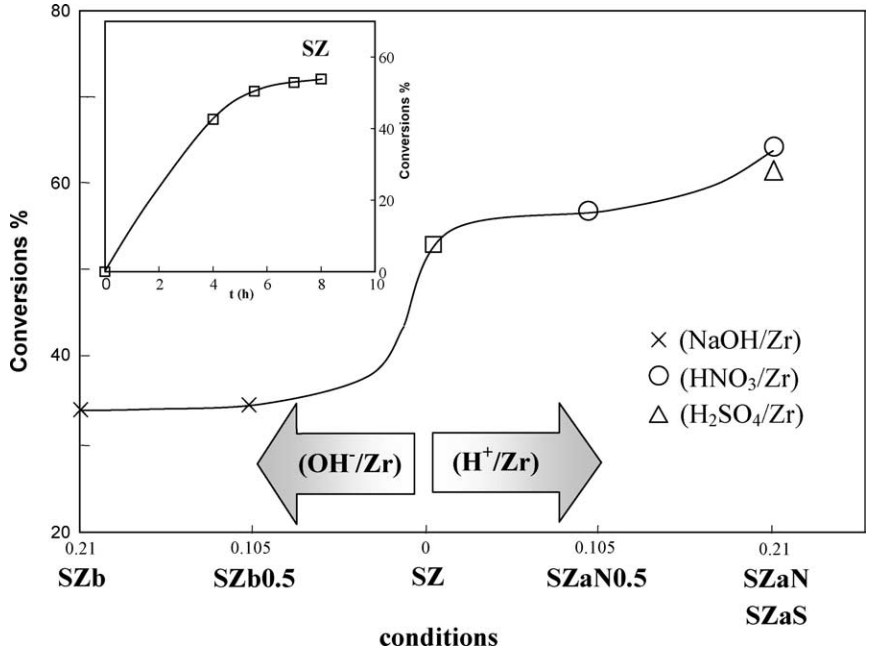

Fig. 6. Reagents conversion for benzoic acid esterification for 8-h reaction time. Inset: reaction profile (conversion vs time) for SZ sample.

attracting power with respect to the metal and consequently a lower catalytic activity of cus (coordinatively unsaturated) Zr^{4+} centers. Further, it can be recalled that SZb, obtained in the most alkaline conditions, shows the largest S/Zr XPS atomic ratio. This occurrence can be considered representative of a lower acidity of this sample with respect to the other present samples. In fact the elimination of the major part of sulfates, localized at the surface, is necessary to allow the development of strong acid sites [2]. Table 2 further reports that the most efficient catalysts, SZaS and SZaN, show the largest OH/Zr atomic ratio, which decreases with decreasing the conversion efficiency. The OH surface density may be representative of the number of Brønsted acid sites present at the surface.

4. Conclusions

SZ samples were prepared by a sol–gel procedure by varying the conditions of the alkoxide hydrolysis and of the subsequent polycondensation steps leading to the gel formation. More specifically conditions of acid or alkaline promotion were adopted with variable $C_{\mathrm{sol-gel}}$/alkoxide molar ratios. Sulfuric acid or ammonium sulfate were used as sulfating agents. The reaction products, dried as xerogels, were calcined at 890 K.

The variation of the synthesis conditions were found not to affect either the structural features or the surface area of the samples. The alkaline-promoted samples showed, however, a larger pore volume with respect to the neutral-acid samples and an appreciable degree of microporosity. XPS analyses showed that for all samples, the shape of the Zr doublet was regular, as expected for samples calcined at temperatures around 850–900 K; the analysis of the sulfur 2p and oxygen 1s peaks showed that the most alkaline SZb sample bears the largest S/Zr atomic ratio, indicative of a lower acidity and that the OH/Zr atomic ratios decreased in passing from the acid to the base-promoted samples.

DRIFTS analyses showed that the surface features were significantly affected by the conditions of the sol–gel reactions. The shape of the spectrum of the alkaline samples suggests the presence of coordinated sulfate with a higher symmetry with respect to those of samples obtained at neutral-acid pH.

A decreasing trend was observed for the catalytic conversion of benzoic acid to methyl benzoate with increasing the pH of the sol–gel hydrolysis and polycondensation stages. Specifically the activity was at the top for the catalysts synthesized under acid conditions and the lowest for the samples prepared at alkaline pH. It is the opinion of the authors that the major component affecting the catalytic activity of the present SZ catalysts is the actual surface state as apparent in the DRIFTS characterization. In the case of the catalysts synthesized at alkaline pH the bond between the sulfates and the oxide surface does not appear to be of a manifold kind as in the case of the acid-neutral samples; consequently the lack of interactions between dissimilar adjacent positions will lead to the formation of less acid surface sites and a lower catalytic activity.

The XPS OH/Zr atomic ratio shows that the total number of Brønsted sites decreases in passing from the acid to the base-promoted samples.

Acknowledgment

Financial support from the Ministry of Education, University, and Research (MIUR, FIRST Funds) is gratefully acknowledged.

References

[1] R.A. Comelli, C.R. Vera, J.M. Parera, J. Catal. 151 (1995) 96.
[2] C. Morterra, G. Cerrato, S. Ardizzone, C.L. Bianchi, M. Signoretto, F. Pinna, Phys. Chem. Chem. Phys. 4 (2002) 3136.
[3] S. Melada, M. Signoretto, S. Ardizzone, C.L. Bianchi, Catal. Lett. 75 (2001) 199.
[4] F.R. Chen, G. Coudurier, J.F. Joly, J.C. Vedrine, J. Catal. 143 (1993) 616.
[5] A. Clearfield, G.P.D. Serrette, A.H. Khazi-Syed, Catal. Today 20 (1994) 295.
[6] S. Ardizzone, C.L. Bianchi, M. Signoretto, Appl. Surf. Sci. 136 (1998) 213C.
[7] J.M.M. Millet, M. Signoretto, P. Bonville, Catal. Lett. 64 (2000) 135.
[8] S. Ardizzone, C.L. Bianchi, E. Grassi, Colloids Surf. 135 (1998) 41.
[9] S. Ardizzone, C.L. Bianchi, Appl. Surf. Sci. 152 (1999) 63.
[10] S. Chokkaram, R. Srinivasan, D.R. Milburn, B.H. Davis, J. Colloid Interface Sci. 156 (1994) 160.
[11] T. Yamaguchi, Appl. Catal. 61 (1990) 1.
[12] D. Milburn, R. Keogh, D.E. Sparks, B.H. Davis, Appl. Surf. Sci. 126 (1998) 11.
[13] K. Ebitani, J. Konishi, H. Hattori, J. Catal. 130 (1991) 257.
[14] S. Ardizzone, C.L. Bianchi, Surf. Interface Anal. 30 (2000) 77.
[15] M.K. Mishra, B. Tyagi, R.V. Jasra, Ind. Eng. Chem. 42 (2003) 5727.
[16] A. Dicko, X. Song, A. Adnot, A. Sayari, J. Catal. 150 (1994) 254.
[17] D. Milburn, R. Keogh, R. Srinivasan, B.H. Davis, Appl. Catal. A 147 (1996) 109.
[18] P. Nascimento, C. Akratopoulon, M. Oszagyan, G. Coudurier, C. Travers, J.F. Joly, J.C. Vedrine, in: L. Guczi, et al. (Eds.), New Frontiers in Catalysis, Elsevier, Amsterdam, 1993, p. 1185.
[19] C. Morterra, G. Cerrato, Phys. Chem. Chem. Phys. 1 (1999) 2825.
[20] C. Morterra, G. Cerrato, F. Pinna, G. Meligrana, Top. Catal. 15 (1) (2001) 53.
[21] G. Strukul, M. Signoretto, F. Pinna, A. Benedetti, G. Cerrato, C. Morterra, in: Advanced Catalysts and Nanostructured Materials, Academic Press, San Diego, 1996.
[22] C.L. Bianchi, S. Ardizzone, G. Cappelletti, Surf. Interface Anal., in press.
[23] T. López, P. Bosch, F. Tzompantzi, R. Gómez, J. Navarrete, E. López-Salinas, M.E. Llanos, Appl. Catal. A 197 (2000) 107.
[24] D.J. Rosenberg, F. Coloma, J.A. Anderson, J. Catal. 210 (2002) 218.
[25] L.B. McCusker, R.B. Von Dreele, D.E. Cox, D. Louer, P. Scardi, J. Appl. Crystallogr. 32 (1999) 36.
[26] R.J. Hill, C.J. Howard, J. Appl. Crystallogr. 20 (1987) 467.
[27] A. Altomare, M.C. Burla, C. Giacovazzo, A. Guagliardi, A.G.G. Moliterni, G. Polidori, R. Rizzi, J. Appl. Crystallogr. 34 (2001) 392.
[28] S. Ardizzone, C.L. Bianchi, V. Ragaini, B. Vercelli, Catal. Lett. 62 (1999) 59.
[29] J.L. Mohanan, S.L. Brock, Chem. Mater. 15 (2003) 2567.

[30] J.A. Anderson, C.A. Fergusson, J. Non-Cryst. Solids 246 (1999) 177.
[31] J.F. Moulder, W.F. Stickle, K.D. Bomben, Handbook of X-ray Photoelectron Spectroscopy, Perkin Elmer, Eden Praire, 1992.
[32] E.E. Platero, M.P. Mentruit, C.O. Arean, A. Zecchina, J. Catal. 162 (1996) 268.
[33] M. Bensitel, O. Saur, J.-C. Lavalley, G. Mabilon, Mater. Chem. Phys. 17 (1987) 249.
[34] M. Bensitel, O. Saur, J.-C. Lavalley, Mater. Chem. Phys. 19 (1988) 147.
[35] K. Nakamoto, Infrared and Raman Spectra of Inorganic and Coordination Compounds, second ed., Wiley Interscience, New York, 1970.
[36] M. Waquif, J. Bachelier, O. Saur, J.-C. Lavalley, J. Mol. Catal. 72 (1992) 127.
[37] M. Benaissa, J.G. Santiesteban, G. Diaz, C.D. Chang, M. Josè-Yacaman, J. Catal. 161 (1996) 694.
[38] J. Deutsch, A. Trunschke, D. Mueller, V. Quaschning, E. Kemnitz, H. Lieske, Catal. Lett. 88 (2003) 9.
[39] T. Okuhara, M. Kimura, T. Nakato, Appl. Catal. A 155 (1997) L9.
[40] M. Kimura, T. Nakato, T. Okuhara, Appl. Catal. A 165 (1997) 227.
[41] T. Vilarino, J.L. Barriada, M.E. Sastre de Vivente, Phys. Chem. Chem. Phys. 3 (2001) 1053.